6-2012

Synthesis of Pure Aragonite by Sonochemical Mineral Carbonation.

Rafael M. Santos
Katholieke Universiteit Leuven, rafael.santos@sheridancollege.ca

Pieter Ceulemans
Katholieke Universiteit Leuven

Tom Van Gerven
Katholieke Universiteit Leuven

SOURCE Citation

Santos, Rafael M.; Ceulemans, Pieter; and Van Gerven, Tom, "Synthesis of Pure Aragonite by Sonochemical Mineral Carbonation." (2012). *Faculty Publications and Scholarship.* Paper 22.
http://source.sheridancollege.ca/fast_chem_publ/22

Accepted Manuscript

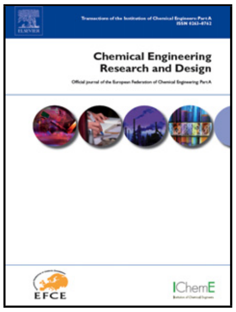

Title: Synthesis of pure aragonite by sonochemical mineral carbonation

Authors: Rafael M. Santos, Pieter Ceulemans, Tom Van Gerven

PII: S0263-8762(11)00477-1
DOI: doi:10.1016/j.cherd.2011.11.022
Reference: CHERD 933

To appear in:

Received date: 21-9-2011
Revised date: 14-11-2011
Accepted date: 29-11-2011

Please cite this article as: Santos, R.M., Ceulemans, P., Van Gerven, T., Synthesis of pure aragonite by sonochemical mineral carbonation, *Chemical Engineering Research and Design* (2010), doi:10.1016/j.cherd.2011.11.022

Graphical Abstract

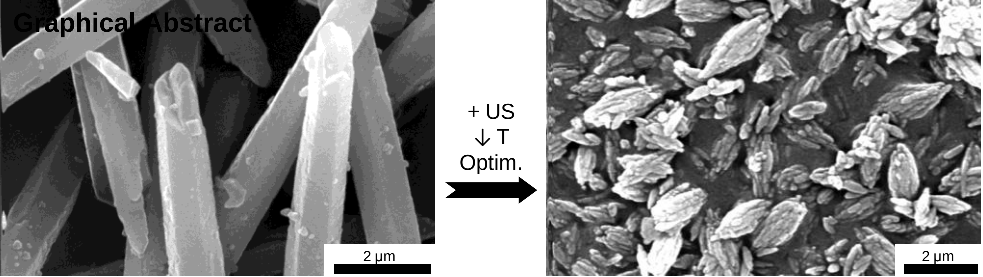

Mechanical mixing, 70 ^{o}C , > 99% aragonite

Ultrasound mixing, 24 ^{o}C, > 98% aragonite

- Ultrasound combined with Mg^{2+} enhances the synthesis of aragonite by carbonation.
- High purity (>98%) aragonite precipitated at 24 ^{o}C with optimized process conditions.
- Influence of several process parameters on product purity explored for optimization.
- Novel aragonite crystal morphology (hubbard squash-like) produced at low temperature.
- Fed-batch process tested as scale-up route for production of pure aragonite powder.

Synthesis of pure aragonite by sonochemical mineral carbonation

*Rafael M. Santos, Pieter Ceulemans, Tom Van Gerven**

Department of Chemical Engineering, Katholieke Universiteit Leuven, B-3001 Leuven, Belgium

*Corresponding author. Tel.: +32 16 322342; Fax: +32 16 322991.
E-mail address: Tom.VanGerven@cit.kuleuven.be (T. Van Gerven)

ABSTRACT

The objective of this work was to promote the formation of the aragonite polymorph of calcium carbonate, which has some valuable applications in industry, via the mineral carbonation route. The combination of ultrasound with magnesium ions promoted the formation of pure aragonite crystals at optimum conditions. It was possible to synthesize high purity aragonite precipitates at temperatures ranging from 24 °C to 70 °C, with the resulting powders possessing varying particle size distributions (from sub-micron up to 20 μm) and crystal morphologies (from acicular needles to novel *hubbard squash-like* particles). Several process parameters were found to influence the produced calcium carbonate polymorph ratios (aragonite over calcite). Higher values of magnesium-to-calcium ratio, intermediate ultrasound amplitude (60%), continuous ultrasound application (100% cycle), introduction of ultrasound pre-breakage, lowering of the CO_2 flow rate, and increase in the relative concentration (g/L $Ca(OH)_2$), all promoted aragonite formation. A potential route for industrial production of this material has been identified via a fed-batch process, which effectively reutilizes magnesium chloride while maintaining high aragonite yield. The results presented herein are significantly superior to aragonite formation using only single promoting techniques, typically found in literature, and go beyond by focusing on pure (>99%) aragonite formation.

Keywords: Calcium carbonate; Polymorph; Aragonite; Mineral carbonation; Ultrasound; Crystal morphology

1. Introduction

Calcium carbonate ($CaCO_3$) is an abundant mineral in nature; approximately 5 % of the Earth's crust consists of it, in the form of limestone (Stearn, 1989). It is an important building material in living organisms as bones, teeth and shells; moreover it can be found in several industrial applications. Calcium carbonate is used as filler or coating pigment in paper, plastics, rubbers and adhesives; as filler, extender and pH buffer in paints; as filler and color stabilizer in concrete; for environmental pollution control and remediation in flue gas and water treatment; in fertilizers and animal feed as calcium supply; among other uses in glass, ceramics, cosmetics and hygienic products (CCA Europe, 2011).

Calcium carbonate appears in nature in three polymorphs. The most common is calcite, as it is the most stable polymorph at ambient temperature and pressure. Its crystal system is trigonal, and appears in a range of morphologies, the most common being rhombohedral and scalenohedral forms (Vecht and Ireland, 2000). Aragonite is a metastable polymorph, commonly occurring in aquatic environments, formed by biological or physical precipitation mediated by suitable pressure, ionic concentration and pH; it can be found in shell structures of shellfish (e.g. oysters and abalones), pearls and sediments in hot springs (Ryu et al., 2010). At standard temperature and pressure, it converts into calcite over several million years. Its crystal system is orthorhombic, and crystals are most commonly needle-like (acicular) or spindle-like, although flower-like (flos-ferri), cauliflower- and flake-like crystals are also reported (Zhou et al., 2004). Lastly, vaterite, which has a hexagonal crystal system and spherical morphology (Wang et al., 1999), is the rarest polymorph, being unstable and rapidly reverting to one of the more stable forms.

Calcium carbonate that is industrially used as a filler or pigment is most commonly calcite due to easy production routes. Aragonite, however, presents some improved physical and mechanical properties. Polyvinyl alcohol or polypropylene composites with aragonite filler show improved tensile strength, impact strength, glass temperature and decomposition temperature (Hu et al., 2009), while aragonite-containing paper coating benefits from improved brightness, opacity, strength and printability (Katayama et al., 1992). Given the differences in material physical properties (Table 1) between the polymorphs are small, the improved aragonite performance is attributable to morphological differences (e.g. particle aspect ratio and packing density).

Aragonite synthesis by mineral carbonation is favored at 60 to 70 °C (Hu and Deng, 2003). At higher temperatures (and ambient pressure), aragonite is unstable and polymorph change towards calcite takes place (Passe-Coutrin et al., 1995). At lower temperatures, such as ambient, vaterite formation is possible; however its conversion to calcite is rapid (Wang et al., 1999). On the other hand, aragonite is calcium carbonate's high-pressure polymorph: increasing the pressure advances the stability of the crystals (Zhou et al., 2004).

Aragonite synthesis can also be promoted by controlling the aqueous chemistry of the precipitation solution, an example being the control of the saturation degree (SS). A low degree of supersaturation ($SS \ll 1$) has been found to favor aragonite formation (Hu and Deng, 2003). Matsumoto et al. (2010) used the minute gas–liquid interface around CO_2/NH_3 microbubbles as a reaction field to promote aragonite nucleation. It was possible to adjust the concentration of Ca^{2+} and CO_3^{2-} ion concentrations at the interface by varying solution pH and gas composition, which affected the electric charge on the bubble surface and the difference between local and bulk pH. At a solution pH of 9.7-10.5 the crystallization of aragonite was accelerated remarkably with a decrease in the CO_2/NH_3 ratio and gas bubble size (<100 μm).

Additionally, additives have been found to enhance aragonite formation in several studies. Ota et al. (1995) was able to obtain aragonite whiskers from the carbonation of a mixture of calcium hydroxide and magnesium chloride, at a molar Mg-to-Ca ratio (MCR) of 1.52, at 80 ^{o}C. Similarly, Katayama et al. (1992) used phosphoric acid as an additive instead of magnesium, at 2 wt% to $Ca(OH)_2$, and obtained 20 μm long aragonite needles at 50 ^{o}C. The most relevant study to date on aragonite synthesis for the carbonation system of interest in the present study is that of Park et al. (2008). They investigated the influence of the concentration of magnesium ions ($MgCl_2$) on the carbonation of $Ca(OH)_2$ slurry in a reactor at 80 °C. It was found that when the magnesium concentration is higher than 71 mol%, corresponding to a magnesium-to-calcium ratio (MCR) greater than 2, pure aragonite can be synthesized. Moreover, increasing the MCR resulted in smaller particles, with a maximal aspect ratio occurring in the interval of 71–75 mol%. They postulated that the magnesium ions bind to the calcite microcrystal surface, inhibiting the nucleation and growth of calcite crystals. In an earlier study, Ahn et al. (2004) had found that aragonite formation had no permanent relation to the pH value, the MRC, or the Mg^{2+}/Ca^{2+} concentrations in solution. It was suggested that synthesis of aragonite requires a concentration of magnesium ions in the appropriate range (0.10–0.26 M) and a concentration of calcium ions below a certain range (< 0.16–0.25 M); otherwise an excess of calcium ions or magnesium ions would favor calcite formation.

Finally, ultrasound (US) has also been seen to promote precipitation of the different polymorphs of calcium carbonate. The use of ultrasound in chemical processes, also termed sonochemistry, applies sound waves in the range of 16 to 100 kHz. Power is delivered to a solution by inducing cavitation, that is, the formation of small cavities or microbubbles that grow and collapse rapidly. The collapsing microbubbles produce high local temperatures and pressures and high shear forces. Experimental work is reported on the use of ultrasound to speed up carbonation of an aqueous calcium carbonate salt solution (Nishida, 2004) and the seeded sonocrystallization of calcite at constant composition conditions (Boels et al., 2011). Rao et al. (2007) found that ultrasound increased the carbonation conversion of fluidized bed combustion ash, and López-Periago et al. (2010) used a sonic bath to enhance carbonation of calcium hydroxide using supercritical CO_2. The formation of vaterite with ultrasound has been reported from aqueous salt solutions (Kojima et al., 2010; Price et al., 2011). Zhou et al. (2004) found pure aragonite to form from $Ca(HCO_3)_2$ solution at 70 ^{o}C with an ultrasound intensity of 58–99 W (in 250 mL) at 20 kHz. The high temperatures and pressures, suitable for aragonite formation, caused by the ultrasound-induced cavitations were attributed to the result. Mateescu et al. (2007) mixed $Ca(NO_3)_2$ drop-wise into a solution of K_2CO_3 in a sonic bath at 40 ^{o}C and obtained preferential formation of aragonite and vaterite when maintaining the pH constant at 10.

Process Intensification (PI) seeks to bring together fundamental aspects of process engineering technology and to find the most optimum balance between them (Santos and Van Gerven, 2011). With a view of finding a PI route to aragonite synthesis by mineral carbonation, the main objectives of this work were:

i. To improve aragonite synthesis by the combined use of ultrasound and chemical additives to promote pure aragonite formation at economical process conditions; emphasis was given to the synthesis of pure aragonite at low temperatures (≤ 30 ^{o}C).

ii. To explore the influencing parameters that induce aragonite formation based on directions given in literature, but herein performed systematically and dedicated to the mineral carbonation process; the aims were to confirm and extend the state of knowledge, and to find the optimum aragonite-promoting process conditions.

2. Experimental Section

For sonication an ultrasonic processor Hielscher UP200S was used, which operates at 24 kHz frequency and delivers 200 W gross power. The probe used was an S14 sonotrode, which has a tip diameter of 14 mm, maximal amplitude of 125 μm, and an acoustic power density of 105 W/cm². A PT100 temperature sensor connected to the device monitored solution temperature. Experiments in slurry were conducted using a laboratory glass beaker with a volume of two liters and diameter of approximately 14 cm; the beaker was filled with one liter of distilled water, reaching a height of 7.5 cm. The probe tip was immersed up to 3.5 cm from the bottom. Typical experiments were performed with 3.7 g/L of $Ca(OH)_2$ solids. The suspension was mixed solely by the ultrasound horn during sonication experiments, or with a mechanical stirrer (Heidolph type RZ-R1) and straight blade impeller at 340 rpm for stirred experiments. CO_2 was delivered to the solution from a compressed gas cylinder with flow controlled by a rotameter (Brooks Sho-rate). Temperature was controlled by use of a hot plate (IKAMAG RCT) for heating and water bath for cooling; because ultrasound produces heat, it must be dissipated to operate at lower temperatures or simply to maintain a constant temperature. The experimental set-up used is illustrated in Fig. 1. The following analytical grade materials were used in this study: $Ca(OH)_2$ (Acros Organics), $MgCl_2 \cdot 6H_2O$ (Chem-Lab), industrial grade CO_2 ≥99.5% (Praxair).

The typical experimental procedure commenced by dissolving the desired amount of magnesium chloride hexahydrate (e.g. 30.5 g/L for MCR = 3) in one liter ultrapure water (18.2 MΩ·cm). Then, the desired amount of calcium hydroxide powder (typically 3.7 g/L, referred to herein as relative concentration (RC) of 1) was poured into the beaker. While mixing (by ultrasound or mechanical agitation), the mixture is heated to the desired temperature, either solely by the ultrasonic device or the hot plate. When the desired temperature is reached, the carbonation reaction is started by bubbling CO_2 gas (typical flow rate 0.24-0.72 NL/min) through the slurry. Carbonation continues until the solution pH reaches a constant value, indicating reaction completion, typically within 30 to 120 minutes. The slurry then is filtered (589/3 filter paper), rinsed, and dried at 105 °C for four hours to recover the calcium carbonate crystals.

Particle size analysis of precipitate samples was determined by laser diffraction (LD) (Malvern Mastersizer S). Morphological assessment was performed by imaging with a scanning electron microscope (SEM) (Philips XL30 FEG). Mineralogical analysis was conducted by X-ray diffraction (XRD) (Philips PW1830), equipped with a graphite monochromator and a gas proportional detector, using Cu Kα radiation at 30 mA and 45 kV, step size of 0.03^{o} 2θ and counting time 2 s per step, over 5 to 70^{o} 2θ range; mineral identification was done in DiffracPlus EVA (Bruker) software.

Quantification of calcite and aragonite in completely carbonated samples was performed using Eq. (1), where F_a is the fraction (wt%) of aragonite and I is the intensity of an associated peak: I_{111} and I_{221} refer to the aragonite peaks at 26.3° and 45.9° 2θ, I_{104} is the intensity of the calcite peak at 29.5°. This equation is derived from the equation used by Park et al. (2008), but fitting the coefficients to calibration performed using pure standards at three aragonite(A):calcite(C) mixture ratios: 25%A:75%C, 55%A:45%C, and 75%A:25%C. The quantification uncertainty is estimated at approximately ±0.5%.

$$F_a = \frac{I_{111} + 0.215 \cdot I_{221}}{I_{111} + 0.215 \cdot I_{221} + 0.472 \cdot I_{104}} \qquad (1)$$

3. Results and Discussion

3.1. Influence of stirring mode and temperature

A combination of the approaches of Park et al. (2008) and Zhou et al. (2004) was used to promote the formation of aragonite from the carbonation of calcium hydroxide powder; that is, both magnesium ions and ultrasound were used in slurry carbonation. The first series of experiments involved testing the hypothesis that ultrasound promotes aragonite synthesis. This was accomplished by comparing the mineralogy of samples carbonated with ultrasound mixing and with mechanical mixing. Furthermore, the temperature of the reaction was varied to find out if aragonite formation is possible at temperatures lower than those reported in literature (70 ^{o}C (Zhou et al., 2004), 80 ^{o}C (Ota et al., 1995; Park et al., 2008)). A magnesium-to-calcium ratio (MCR) of 3 was chosen for these experiments (according to the MCR > 2 criteria of Park et al. (2008)).

Fig. 2 shows XRD diffractograms of the synthesized precipitates at the four temperatures using mechanical mixing (left) and ultrasound mixing (right). At 70 °C, essentially pure aragonite (>99%) is formed with both mixing methods. Lowering the reaction temperature elevates the calcite content. At 55 °C with mechanical mixing the amount of calcite is still small, but at lower temperatures (40 °C and 30 °C) the calcite phase becomes dominant. Based on the peak heights at 55 ^{o}C and the data presented in Table 2, it appears >99% aragonite can be obtained at temperatures just slightly higher. These results suggest a slight improvement with regards to synthesis temperature in comparison with results of Ota et al. (1995) and Park et al. (2008), and confirm the effect of temperature on promoting aragonite formation in the presence of magnesium ions.

The effect of ultrasound on aragonite formation is confirmed by comparison with the mechanical agitation results in Fig. 2. It is evident that at every temperature lower than 70 ^{o}C the amount of aragonite is greater with use of ultrasound. Moreover, at 30 ^{o}C and 40 ^{o}C aragonite remains as the dominant polymorph when using ultrasound, compared to nearly complete reversal to calcite (and magnesian-calcite at 30 ^{o}C inferred from the double peak at 29.5–30^{o}) with mechanical mixing. These results are reaffirmed by the quantitative analysis reported in Table 2. At 55 ^{o}C essentially pure aragonite (99.6%) is formed with ultrasound. It is clear that the use of ultrasound in the presence of magnesium ions allows for pure aragonite formation at lower temperatures than reported by Zhou et al. (2004).

It is believed that the cavitations formed by the use of ultrasound introduce two effects that promote the formation of aragonite. First, the imploding cavities generate localized, micron-sized or smaller, regions of high temperature, even though the bulk solution temperature may be fixed at a low value (e.g. 30 ^{o}C). Since aragonite formation is promoted at higher temperatures, it can be expected that these high temperature regions, even if in existence for fractions of a second, lead to the nucleation of aragonite seeds, which then can grow into larger aragonite crystals at bulk solution temperatures. Second, the generation of nucleation sites is likely greatly enhanced by sonication, therefore even if crystal growth of aragonite at lower bulk temperature is comparatively slow, the constant generation of aragonite seeds enables aragonite crystal growth to remain statistically preferable over calcite. These mechanisms can also explain the morphological differences seen in the precipitates, discussed next.

The morphology of the crystals produced is illustrated in Fig. 3 for eight cases: ultrasound at four different temperatures: 70 ^{o}C (a), 55 ^{o}C (b), 40 ^{o}C (c), 30 ^{o}C (d); and mechanical mixing at four different temperatures: 70 ^{o}C (e), 55 ^{o}C (f), 40 ^{o}C (g), 30 ^{o}C (h). The aragonite contents of these samples correspond to the letter-indexed values listed in Table 2. It can be clearly seen that at 70 ^{o}C the particle morphology resembles needle-like aragonite reported in literature, regardless of mixing method. Also with both mixing methods, lowering temperature results in reduction of particle size. However with ultrasound mixing, the particles remain aragonite, achieving newly observed particle morphology at 30 ^{o}C (*hubbard squash-like*), shown in more detail on Fig. 4. As aforementioned, these smaller aragonite crystals may be a product of slower aragonite crystal growth at lower temperatures, combined with increased aragonite nucleation in the presence of ultrasound. The *hubbard squash-like* morphology can also be seen in selected particles in Fig. 3h, achieved with mechanical mixing; however in this case scalenohedral calcite crystals are dominant. This further reaffirms that the unique morphology is due to synthesis at low temperature rather than solely due to sonication of the forming crystals.

The images in Fig. 3b, Fig. 3c, Fig. 3f and Fig. 3g show transitionary crystal morphologies. With ultrasound, the crystals at 55 ^{o}C still resemble needles but become scaly, while with mechanical mixing the needle-like particles appear more degraded and have lower aspect ratio. At 40 ^{o}C, ultrasound mixing yields particles that begin to resemble the low temperature morphology, but having larger size. In comparison, the 40 ^{o}C mechanical mixing sample is composed of a mixture of aragonite particles similar to those at 55 ^{o}C but smaller, and nano-sized calcite crystals both of rhombohedral and scalenohedral morphologies.

3.2. Influence of MCR

In an ultrasonic environment with an MCR of 3, pure aragonite can be synthesized at 55 °C, as shown previously. It was of interest to know if a higher MCR allows for production of pure aragonite at lower temperatures (30 ^{o}C). Also, it was of interest to know if an optimal MCR exists at different temperatures (i.e. can the MCR be lowered at 55 ^{o}C while still obtaining >99% aragonite). Carbonation experiments were conducted by varying the MCR between 0 and 6, at 30 ^{o}C and 55 ^{o}C, with use of ultrasound mixing in $Ca(OH)_2$ slurry as described previously. Fig. 5 presents the aragonite content of the calcium carbonate precipitates produced. Aragonite was more easily formed at higher temperature; at 55 °C, pure aragonite can be synthesized with MCR = 2.5, whereas at 30 °C an MCR = 6 is necessary. Already with MCR = 1 it is possible to synthesize over 50% aragonite at 55 ^{o}C, and over

90% at MCR = 1.5; similar results are only achieved at 30 °C with a half unit greater MCR. It is concluded that there is in fact an optimal MCR for each temperature. Moreover it is proven possible to synthesize pure aragonite close to room temperature at optimized conditions.

Additionally, a possible explanation of the mechanism of magnesium ions in participating in the carbonation reaction to promote aragonite was observed. Upon addition of magnesium chloride to solution, magnesium ions reacted with water and precipitated as brucite ($Mg(OH)_2$). Brucite formation was found to be quite fast, as evidence by large brucite peaks in XRD analysis for samples filtered minutes after mixing. Furthermore, unreacted portlandite peaks were found to nearly disappear, indicating that calcium ions had been leached into solution, forming dissolved calcium chloride (Eq. 2). Over time, it is believed that as calcium ions react with carbonate ions, brucite solubilizes back into magnesium chloride, and calcium carbonate is precipitated (Eq. 3). This is also confirmed by reduction in brucite peak heights by XRD, and complete disappearance once the carbonation reaction is completed. These reaction steps were confirmed by Visual MINTEQ chemical equilibrium modeling and are presented in more detail in Ceulemans (2011). The promotion of aragonite in the presence of magnesium chloride thus may be linked with the carbonation reaction taking place in solution rather than by direct mineral carbonation (Eq. 4).

$$Ca(OH)_2 + MgCl_{2(aq)} \rightarrow Mg(OH)_2 + CaCl_{2(aq)} \qquad (2)$$

$$CaCl_{2(aq)} + CO_{2(aq)} + Mg(OH)_{2(aq)} \rightarrow CaCO_3 + H_2O + MgCl_{2(aq)} \qquad (3)$$

$$Ca(OH)_2 + CO_{2(aq)} \rightarrow CaCO_3 + H_2O \qquad (4)$$

3.3. Influence of ultrasound parameters

The ultrasound probe used allows the setting of two process parameters: amplitude and cycle. The amplitude is the distance the sonotrode surface travels within an oscillation stroke. Larger amplitude leads to higher rate at which the cavity pressure increases and decreases at each stroke, and increased displacement volume, resulting in a larger cavitation volume (bubble size and/or number). When applied to slurries, higher amplitudes provide greater potential for solid particle breakage (Hielscher, 2006). Amplitude is expressed as a percentage of the maximum amplitude (125 μm). Cycle refers to the fraction of experimental time during which sonication is applied. The ultrasound can be used in such way that the sonication is pulsed on and off in short time intervals. Cycle is expressed as a percentage of total experimental time. Previous experiments were performed with 100% amplitude and cycle. In this section, experiments are executed at an intermediate MCR value (1.5 at 30 ^{o}C) so that the effect of varying amplitude and cycle on aragonite fraction can be investigated. The objective is the optimum ultrasound setting that maximizes aragonite content.

Fig. 6 shows the effect of amplitude and cycle on aragonite synthesis. Using either cycles of 20% and 100%, there is a maximum aragonite fraction at an intermediate amplitude (60%). Higher cycle (100%), meaning more ultrasound use, also leads to greater aragonite synthesis. Therefore the optimal configuration is found to be 60% amplitude and 100% cycle. Zhou et al. (2004) also found intermediate amplitudes to favor aragonite. However in their case the competing polymorph at higher amplitudes was vaterite; vaterite was not detected in this work.

The reason for intermediate amplitudes being optimal may lie in the effect of ultrasound intensity on the generation rate of cavities and their resulting collapse pressure (Gogate et al., 2003). Gogate et al. (2003) have found by computational modeling that although an increase in ultrasound intensity leads to bubble growth, it also leads to a reduction of the bubble wall pressure at the collapse point of the cavity, due to dissipation of energy from the longer-living bubble to the liquid medium. They postulate that upon increasing intensity, there is an optimal point where the overall pressure pulse, defined as the product of the number of cavities in the system and the collapse pressure due to the single cavity, is greatest, beyond which it decreases due to leveling off of cavity generation. For the present system (i.e. ultrasonic processor, sonotrode probe, 1 liter water medium volume, and 2 liter glass beaker receptacle) it may well be that the optimal overall pressure pulse occurs near 60% amplitude.

3.4. Influence of other process parameters

Three additional process parameters were investigated for their effect on aragonite formation: ultrasound pre-breakage, CO_2 flow rate, and relative concentration. Results are shown in Table 3 for varying sets of process conditions.

Pre-breakage is defined as sonication time applied to the calcium hydroxide slurry prior to CO_2 gas introduction into the solution. The objective is to reduce the particle size induced by the imploding cavitations, thereby increasing uncarbonated material surface area, which should have an effect both on the dissolution and the carbonation reaction kinetics and equilibria. Table 3 presents four sets of data, comparing samples subjected or not to pre-breakage (from 0 to 45 minutes). These sets utilize varying process conditions (pre-breakage times, MCR, mixing, relative concentration and CO_2 flow). It can be seen that under all process condition combinations, save the last, pre-breakage promotes greater aragonite synthesis, expressed as the aragonite fraction of the resulting calcium carbonate precipitates. In the first two cases the benefit is greater given the process conditions lead to intermediate aragonite purity, while for the later two cases the benefit is smaller to nil, given aragonite purity is greater than 90% already. It is theorized that pre-breakage promotes aragonite synthesis by improving the reaction between calcium hydroxide and magnesium chloride prior to carbonation, whereas without pre-breakage there is greater likelihood that calcium ions dissolved directly from unreacted calcium hydroxide will form calcite.

The next process parameter discussed is CO_2 flow rate. Table 3 presents results from two series of experiments conducted with varying CO_2 flow rate, and identical remaining parameters. It is found that increasing the CO_2 flow rate leads to greater calcite formation, whereas lowering the CO_2 flow rate promotes aragonite; this result is particularly noticeable with mechanical mixing, where the aragonite content increases from 20.4% to 91% at MCR = 3 and 30 ^{o}C. This effect can be directly linked to reaction time. As shown in Fig. 7, with a flow rate of 0.72 NL/min the reaction is completed (pH drop levels off) in approximately 50min, while at 0.24 NL/min and 0.12 NL/min the reaction is completed only after 2h15min and 4h30min, respectively. It is thought that the lower CO_2 flow rate leads to a lower level of solubilized CO_2 (i.e. under saturation), decreasing the probability of carbonate ions reacting with calcium ions leached directly from $Ca(OH)_2$, rather than the dissociated calcium chloride species. These results are in agreement with those of Hu and Deng (2003), who found a low degree of supersaturation to promote aragonite synthesis. However in comparison, aragonite fractions in the present study are much higher than those reported therein (~20% at 36 ^{o}C), which were synthesized from sparingly soluble calcium salts.

Lastly, the effect of relative concentration (RC) on aragonite formation was tested. Relative concentration is defined as the initial calcium hydroxide concentration in slurry relative to the typical value of 3.7 g/L used in most experiments (e.g. RC = 2 means $Ca(OH)_2$ = 7.2 g/L). It should be noted that the magnesium chloride concentration is adjusted accordingly to maintain the same MCR for comparison purpose. Table 3 presents two sets of experiments where RC was varied; process parameters such as MCR, US amplitude and CO_2 flow rate differ between these two sets. It is found that lower RC is detrimental to aragonite formation in both cases. In fact, by doubling the relative concentration for the first series, the aragonite content at 30 ^{o}C nearly reaches 99%, compared to just under 93% at typical concentrations and MCR = 3. In this case, the aragonite promoting effect may be linked to the increased magnesium chloride concentration when RC is larger. Increasing the concentration of $Ca(OH)_2$ should not significantly change the rate or extent of calcium dissolution, given all slurries are over-saturated with respect to $Ca(OH)_2$. As a result, by maintaining the MCR constant, the concentration of soluble chloride species, both Mg and Ca, significantly increases, thereby increasing the effective influence of magnesium chloride (i.e. at RC = 2 and MCR = 3, it is as if the MCR was 6). These results are in agreement with observations of Ahn et al. (2004), who postulated that magnesium concentration rather than MCR controls aragonite formation, with a minimum Mg concentration being required to suppress calcite formation. Along these lines, in Table 3 it can be seen that when RC = 1/2 or 1/3 the aragonite fractions drops significantly. A last note to be made about relative concentration is that the carbonation reaction time decreases at lower RC, as can be seen in Fig. 7 for RC = 1/3. This finding will be used later on in the section about a fed-batch process.

3.5. Synthesis at optimized conditions and lowest temperature

Up to this point, investigating and optimizing influencing parameters has resulted in a list of optimal values, which can be combined to improve the low-temperature synthesis of aragonite. Of particular note, rather than using RC = 2 with MCR = 3, it was chosen to keep RC = 1 with MCR = 6, to reduce the reaction time. Also the CO_2 flow rate chosen was 0.24 NL/min, again to reduce the reaction time compared to using the 0.12 NL/min found to be optimal for aragonite selectivity. The final combination conditions utilized for the optimized synthesis, which resulted in 99.0% aragonite precipitate with the morphology shown in Fig. 8a, were:

- T = 30 °C
- RC = 1
- MCR = 6 (3.7 g $Ca(OH)_2$ + 61 g $MgCl_2.6H_2O$ in 1 liter DI water)
- US Amplitude = 60%; US Cycle = 100%

- CO_2 flow = 0.24 NL/min
- PB = 20 minutes

A final attempt was made to reduce the synthesis reaction even further. The reaction temperature was lowered to 24 °C, and more severe aragonite-favoring conditions were chosen: MCR = 8 and CO_2 flow = 0.12 NL/min. While the reaction time was rather long (4.5 hours), the aragonite purity obtained was very satisfactory: 98.6%. The crystal morphology is shown in Fig. 8b, possessing the unique *hubbard squash-like* shape. The XRD pattern of this sample is compared to that at 30 ^{o}C in Fig. 9, both being essentially identical except for slightly higher I_{111}:I_{021}, I_{112}:I_{022} and I_{141}:I_{113} ratios at 24 ^{o}C.

3.6. Fed-batch process

To make this synthesis process interesting from an industrial production perspective the efficiency of this process must be higher. Indeed, in 1 liter water at RC = 1 there will be only five grams of aragonite produced according to this process. Furthermore, for synthesizing those five grams, 61 g of magnesium chloride hexahydrate are needed. This ratio appears wasteful, unless the magnesium chloride can be proven to be reusable. Two ideas were considered: (i) filtering the carbonated slurry and reutilizing the solution for further synthesis cycles with addition of new $Ca(OH)_2$, or (ii) adding new $Ca(OH)_2$ to the synthesis slurry on a continuous basis for an extended period of time (i.e. a fed-batch process (Ahn et al., 2007)). The second solution turned out to be the preferred route, as in the first case the filtration proved difficult to perform in a timely manner and the synthesis product suffered from contamination with brucite ($Mg(OH)_2$) when the reaction had not been fully completed prior to filtration (Ceulemans, 2011). The following process conditions were chosen for the fed-batch process:

- T = 30 °C
- $Ca(OH)_2$ = 1.2 g every 12 minutes

- Mg = 61 g $MgCl_2.6H_2O$, one time addition, in 1 liter DI water
- Time = 144 minutes (12 additions)
- US Amplitude = 60 %; US Cycle = 100 %

The resulting fed-batch-produced calcium carbonate precipitate contained 96.7% aragonite, as shown in Fig. 9. The cause of the small calcite formation is possibly due to addition of fresh $Ca(OH)_2$ directly to the slurry during carbonation, while in previous single batch experiments the calcium hydroxide was pre-mixed with magnesium chloride prior to CO_2 introduction. A small portion of the newly added $Ca(OH)_2$ may react directly with carbonate ions forming calcite, prior to magnesium chloride taking its full effect in equilibrating with the unreacted material. The aragonite purity may improve further if $Ca(OH)_2$ addition is done in a truly continuous basis with a feeding pump. The particle morphology also changed from the *hubbard squash-like* shape to what appear to be clustered crystal particles of 1-3 μm in size. By inspection of Fig. 8c, it appears additional crystal growth occurs due to prolonged exposure of early-synthesized aragonite crystals to the reacting slurry. Maintenance of the *hubbard squash-like* likely requires immediate separation of the formed crystals prior to solution re-utilization.

3.7. Precipitate powder characterization by laser diffraction

Pure aragonite precipitates were synthesized in this study at a range of temperatures spanning from 24 ^{o}C to 70 ^{o}C. As has been shown by SEM analysis (Fig. 3), particle morphology changes as a function of temperature and so does particle size. Particle size and particle size distribution are important parameters of powder materials for certain industrial applications such as paper coating or polymer filler; these data are not typically reported in literature for novel calcium carbonate morphologies, making it impractical to assess their suitability for industrial use. As such, the effect of synthesis temperature on aragonite particle size was studied in more detail by laser diffraction.

Table 4 lists average particle sizes by volume, expressed as D50 (mean volume diameter), D[3,2] (surface area moment mean diameter) and D[4,3] (volume moment mean diameter), and Fig. 10 shows the volume-based size distributions. All samples were synthesized with ultrasound and contain greater than 98% aragonite as indicated. In general, lowering the synthesis temperature results in shifting of the distribution to the left (smaller sized). This is confirmed in Table 4 for the three listed size averages. The distributions of precipitates synthesized at higher temperatures have bimodal/trimodal characteristics, having a primary peak between 1 μm and 20 μm (and an intermediate peak at 2 μm for the 70 ^{o}C case) and a secondary peak below 1 μm. The larger mode likely represents the needle-shaped particles, while the smaller modes may be fragmented particles, due to sonication, and/or particles that formed near the end of the experiments when crystal growth could be hindered by diminishing calcium concentration in solution. Samples from low temperature synthesis (24 ^{o}C and 30 ^{o}C) have unimodal distributions below 3 μm. The low temperatures, which may hinder crystal growth throughout the experiment, could be attributed to the smaller particle sizes. The fed-batch sample was found to have a bimodal distribution, likely comprised, as suggested by SEM images, of larger clustered crystals and smaller ultrasound-cleavaged particles.

4. Conclusions

Ultrasound has been proven, in combination with magnesium chloride in solution, to enhance the synthesis of aragonite crystals by mineral carbonation, both by reducing the required concentration of magnesium and reducing the required reaction temperature to near ambient conditions. While in literature the synthesis temperature of aragonite normally is situated in the 60 ^{o}C to 90 ^{o}C range, in the present work high purity aragonite precipitates were produced even at 24 ^{o}C using a combination of optimized process parameters found by application of the principles of Process Intensification.

The effect of several process parameters on aragonite synthesis was systematically studied beyond temperature, including the magnesium-to-calcium ratio (MCR), ultrasound (US) settings (amplitude and cycle), US pre-breakage (PB), CO_2 flow rate, and relative concentration (RC). It was found that higher values of MCR promoted aragonite, but in the presence of ultrasound the MCR corresponding to a similar level of aragonite fraction of the carbonate precipitates decreased in comparison with standard mechanical mixing. An intermediate ultrasound amplitude (60%) was most beneficial to aragonite promotion at intermediate MCR levels, similar to reported observations by Zhou et al. (2004), while aragonite purity was proportional to ultrasound application, with 100% cycle (continuous US) being best. Ultrasound pre-breakage is theorized to promote aragonite synthesis by improving the reaction between calcium hydroxide and magnesium chloride prior to carbonation, reducing the likelihood that calcium ions dissolved directly from unreacted calcium hydroxide will form calcite. Lowering the CO_2 flow rate was also found to promote aragonite synthesis, leading to lower level of supersaturation that has been reported to favor aragonite (Hu and Deng, 2003). Finally the aragonite promoting effect of relative concentration was linked to the increased magnesium chloride concentration when RC is larger, though the MCR remains the same; this response has also been previously suggested by Ahn et al. (2004).

While other authors have reported similar strategies to promote aragonite, none have combined them to find an optimal process that produces pure aragonite; in fact most studies only report aragonite production at low purity levels or even in near trace amounts. That is why the reaction temperature is typically kept relatively high. In this work not only low temperature aragonite synthesis was proven, but crystals with new particle morphology (*hubbard squash-like*) have been produced. This material may have interesting industrial applications, which are yet to be identified. A potential route for industrial production of nearly pure aragonite at low temperature has been identified via a fed-batch process, which effectively reutilizes magnesium chloride while maintaining high aragonite yield, though the crystal morphology changes due to prolonged ultrasound exposure and clustered crystal growth.

Acknowledgements

The K.U.Leuven Industrial Research Fund (IOF) is gratefully acknowledged for funding the Knowledge Platform on Sustainable Materialization of Residues from Thermal Processes into Products (SMaRT-Pro²) in which this work was performed. R.M.S is thankful for the PGS-D support from the Natural Sciences and Engineering Research Council of Canada (NSERC). The K.U. Leuven Department of Earth and Environmental Sciences and the Department of Metallurgy and Materials Engineering are acknowledged for the use of XRD, LD, and SEM equipment. Special regards to Dr. Gilles Mertens (Qmineral) for XRD measurement and interpretation assistance.

References

Ahn, J.-W., Choi, K.-S., Yoon, S.-H., Kim, H., 2004. Synthesis of Aragonite by the Carbonation Process. J. Am. Ceram. Soc. 87, 286–288.

Ahn, J.-W., Kim, J.-H., Ko, S.-J., 2007. Novel Manufacturing Method of Aragonite Calcium Carbonate. WIPO Patent 2007/078017, July 12, 2007.

Boels, L., Wagterveld, R.M., Mayer, M.J., Witkamp, G.J., 2010. Seeded calcite sonocrystallization. J. Cryst. Growth 312, 961–966.

CCA Europe, 2011. Mineral applications. http://www.cca-europe.eu/mineral-applications.html (accessed 07/13/2011).

Ceulemans, P., 2011. Improved synthesis of aragonite. M.Sc. Thesis, Katholieke Universiteit Leuven, July, 2011.

Dimmick, A., 2003. Influence of the average particle size of aragonitic precipitated calcium carbonate on coated paper properties. In Proceedings of TAPPI 2003 Spring Technical Conference and Exhibit and 8th Advanced Coating Fundamentals Symposium, Chicago, USA, 11–15 May 2003.

Gogate, P.R., Wilhelm, A.M., Pandit, A.B., 2003. Some aspects of the design of sonochemical reactors. Ultrason. Sonochem. 10, 325–330.

Haynes, W.M., 2011. CRC Handbook of Chemistry and Physics, 91st Edition, CRC Press/Taylor and Francis, Boca Raton.

Hielscher, T., 2006. Ultrasound as a processing technology for the production of nanomaterials. In Proceedings of Micro & Nano Encapsulation, London, UK, 16–17 February 2006.

Hu, Z., Deng, Y., 2003. Supersaturation control in aragonite synthesis using sparingly soluble calcium sulfate as reactants. J. Colloid Interface Sci. 266, 359–365.

Hu, Z., Shao, M., Cai, Q., Ding, S., Zhong, C., Wei, X., Deng, Y., 2009. Synthesis of needle-like aragonite from limestone in the presence of magnesium chloride. J. Mater. Process. Technol. 209, 1607–1611.

Katayama, H., Shibata, H., Fujiwara, T., 1992. Process for producing aragonite crystal form calcium carbonate with acicular shape. US Patent 5,164,172, November 17, 1992.

Kojima, Y., Yamaguchi, K., Nishimiya, N., 2010. Effect of amplitude and frequency of ultrasonic irradiation on morphological characteristics control of calcium carbonate. Ultrason. Sonochem. 17, 617–620.

López-Periago, A.M., Pacciani, R., García-González, C., Vega, L.F., Domingo, C.J., 2010. A breakthrough technique for the preparation of high-yield precipitated calcium carbonate. Supercrit. Fluids 52, 298–305.

Mateescu, C.D., Mocioi, M., Sarbu, C., Branzoi, F., Chilibon, I., 2007. Morphology of $CaCO_3$ Precipitated in Ultrasonic Field. AIP Conf. Proc. 899, 626.

Matsumoto, M., Fukunaga, T., Onoe, K., 2010. Polymorph control of calcium carbonate by reactive crystallization using microbubble technique. Chem. Eng. Res. Des. 88, 1624–1630.

Nishida, I., 2004. Precipitation of calcium carbonate by ultrasonic irradiation. Ultrason. Sonochem. 11, 423–428.

Ota, Y., Inui, S., Iwashita, T., Kasuga, T., Abe, Y., 1995. Preparation of Aragonite Whiskers. J. Am. Ceram. Soc. 7, 1983–1984.

Park, W.K., Ko, S.-J., Lee, S.W., Cho, K.-H., Ahn, J.-W., Han, C., 2008. Effects of magnesium chloride and organic additives on the synthesis of aragonite precipitated calcium carbonate. J. Cryst. Growth 310, 2593–2601.

Passe-Coutrin, N., N'Guyena, Ph., Pelmard, R., Ouensanga, A., Bouchon, C., 1995. Water desorption and aragonite-calcite phase transition in scleractinian corals skeletons. Thermochim. Acta 265, 135–140.

Price, G. J., Mahon, M.F., Shannon, J., Cooper, C., 2011. Composition of Calcium Carbonate Polymorphs Precipitated Using Ultrasound. Cryst. Growth Des. 11, 39–44.

Rao, A., Anthony, E.J., Jia, L., Macchi, A., 2007. Carbonation of FBC ash by sonochemical treatment. Fuel 86, 2603–2615.

Roberts, W.L., Campbell, T.J., Rapp, G.R., 1990. Encyclopedia of Minerals, 2nd Edition, Van Nostrand Reinhold, New York.

Ryu, M., Kim, H., Lim, M., You, K., Ahn, J., 2010. Comparison of Dissolution and Surface Reactions Between Calcite and Aragonite in L-Glutamic and L-Aspartic Acid Solutions. Molecules 15, 258–269.

Santos, R.M., Van Gerven, T., 2011. Process Intensification Routes for Mineral Carbonation. Greenhouse Gas Sci. Technol. DOI: 10.1002/ghg.36.

Stearn, C.W., Carroll, R.L., 1989. Paleontology - The Record of Life, John Wiley & Sons, New York.

Vecht, A., Ireland, T.G., 2000. The role of vaterite and aragonite in the formation of pseudo-biogenic carbonate structures: Implications for Martian exobiology. Geochim. Cosmochim. Acta 64, 2719–2725.

Wang, L., Sondi, I., Matijevic, E., 1999. Preparation of Uniform Needle-Like Aragonite Particles by Homogeneous Precipitation. J. Colloid Interface Sci. 218, 545–553.

Zhou, G.-T., Yu, J.C., Wang, X.-C., Zhang, L.-Z., 2004. Sonochemical synthesis of aragonite-type calcium carbonate with different morphologies. New J. Chem. 28, 1027–1031.

Tables and Table Captions:

Table 1 - Physical properties of calcite and aragonite (Dimmick, 2003; Haynes, 2011; Roberts et al., 1990).

Property	Calcite	Aragonite
Solubility product (K_{sp})	$3.36{\cdot}10^{-9}$	$6{\cdot}10^{-9}$
Density (g/cm^3)	2.71	2.93
Hardness (Mohs scale)	3	3.5-4
Refractive index	1.58	1.63
Coordination number	6	9

Table 2 - Aragonite fractions as function of agitation method and temperature. MCR = 3, US amplitude/cycle = 1, RC = 1, CO_2 = 0.72 NL/h; letter-indexes (a–f) refer to images in Fig. 3.

Temperature	Ultrasound mixing	Mechanical mixing
70 °C	99.6% (a)	99.5% (e)
55 °C	99.6% (b)	98.7% (f)
40 °C	96.9% (c)	44.6% (g)
30 °C	92.7% (d)	20.4% (h)

Table 3 - Effect of US pre-breakage, CO_2 flow rate and relative concentration on aragonite fractions for various process conditions.

Pre-breakage time (min)	MCR	Temperature (°C)	Mixing	Relative Conc. (w/w)	CO_2 Flow (NL/min)	Aragonite Fraction
Effect of US pre-breakage						
0	1.5	30	60% US	1/3	0.24	**40.4%**
20	1.5	30	60% US	1/3	0.24	**55.6%**
0	1.5	30	60% US	1	0.72	**25.4%**
45	1.5	30	60% US	1	0.72	**41.5%**
0	3	30	Mech	1	0.24	**91.0%**
45	3	30	Mech	1	0.24	**93.0%**
0	6	30	60% US	1	0.24	**99.3%**
20	6	30	60% US	1	0.24	**99.0%**
Effect of CO_2 flow rate						
0	1.5	30	60% US	1	**0.72**	**64.5%**
0	1.5	30	60% US	1	**0.24**	**68.9%**
0	1.5	30	60% US	1	**0.12**	**74.7%**
0	3	30	Mech	1	**0.72**	**20.4%**
0	3	30	Mech	1	**0.24**	**91.0%**
Effect of relative concentration						

0	3	30	100% US	**2**	0.72	**98.8%**
0	3	30	100% US	**1**	0.72	**92.7%**
0	3	30	100% US	**1/2**	0.72	**75.0%**
0	1.5	30	60% US	**1**	0.24	**68.9%**
0	1.5	30	60% US	**1/3**	0.24	**40.4%**

Table 4 - Average particle sizes of pure aragonite synthesized with ultrasound at different temperatures.

Temperature ^{o}C	D50 μm	D[3,2] μm	D[4,3] μm	Aragonite %
70 ^{o}C	4.15	1.31	6.48	99.5%
55 ^{o}C	1.33	0.78	1.87	98.7%
40 ^{o}C	0.98	0.65	1.27	98.6%
30 ^{o}C	0.85	0.69	1.23	99.3%
24 ^{o}C	0.84	0.79	1.09	98.6%
Fed-batch (30 ^{o}C)	1.74	0.87	2.22	96.7%

Figure captions:

Fig. 1 - Schematic overview of mechanically mixed (A) and ultrasound mixed (B) slurry carbonation experimental set-ups.

Fig. 2 - Calcium carbonate polymorphism, determined by XRD, as a function of agitation method (mechanical, A; ultrasound, B) and temperature. MCR = 3, US amplitude/cycle = 1, RC = 1, CO_2 = 0.72 NL/h; Δ = aragonite, ☾ = calcite.

Fig. 3 - Comparison of $CaCO_3$ crystal morphology as a function of carbonation process conditions: (a) US 70 °C, >99% aragonite; (b) US 55 °C, >99% aragonite; (c) US 40 °C, 97% aragonite; (d) US 30 °C, 93% aragonite; (e) mechanical 70 °C, >99% aragonite; (f) mechanical 55 °C, 99% aragonite; (g) mechanical 40 °C, 45% aragonite; (h) mechanical 30 °C, 20% aragonite.

Fig. 4 - Close-up image of *hubbard squash-like* aragonite crystal formed at low temperature (30 ^{o}C).

Fig. 5 - Aragonite fractions as function of MCR and temperature using ultrasound. US amplitude/cycle = 1, RC = 1, CO_2 = 0.72 NL/h.

Fig. 6 - Aragonite fractions as function of ultrasound parameters (amplitude and cycle). MCR = 1.5, T = 30 ^{o}C, RC = 1, CO_2 = 0.72 NL/h.

Fig. 7 - Carbonation kinetics, expressed in pH, as a function of CO_2 flow rate; MCR = 1.5, 30 ^{o}C. 60% US, 0’ PB.

Fig. 8 - Particle morphology at optimized synthesis conditions: (a) 30 ^{o}C; (b) 24 ^{o}C; (c) fed-batch.

Fig. 9 - Mineral analysis by XRD of precipitates produced at optimized aragonite synthesis conditions; ∆ = aragonite fraction.

Fig. 10 - Particle size distributions of pure aragonite precipitates at varying temperatures.

Figure 1

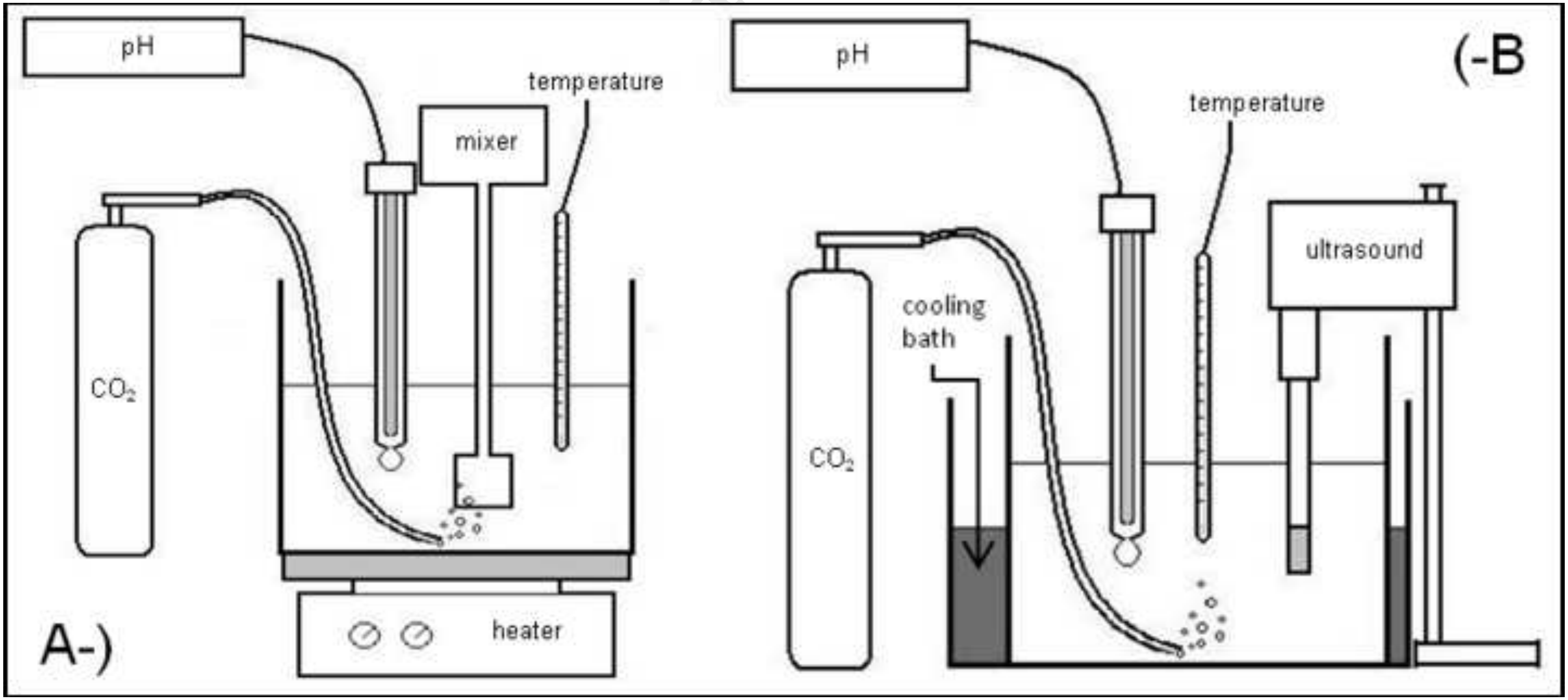
pH
temperature
mixer
CO_2
heater
A-)
pH
(-B
temperature
ultrasound
cooling bath
CO_2

Figure 2

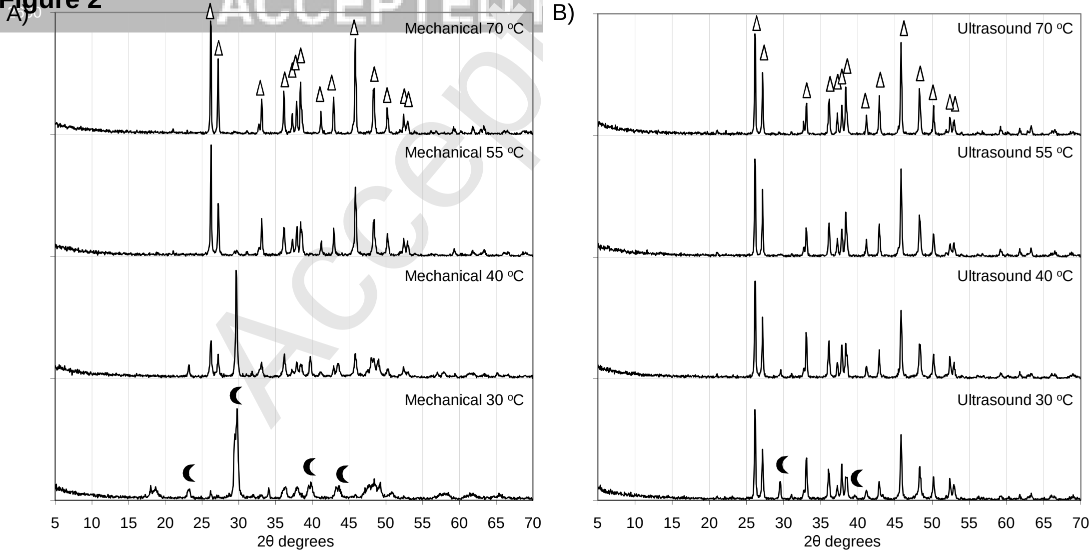
A)
Mechanical 70 ºC
Mechanical 55 ºC
Mechanical 40 ºC
Mechanical 30 ºC
5
10
15
20
25
30
35
40
45
50
55
60
65
70
2θ degrees
B)
Ultrasound 70 ºC
Ultrasound 55 ºC
Ultrasound 40 ºC
Ultrasound 30 ºC
5
10
15
20
25
30
35
40
45
50
55
60
65
70
2θ degrees

Figure 3

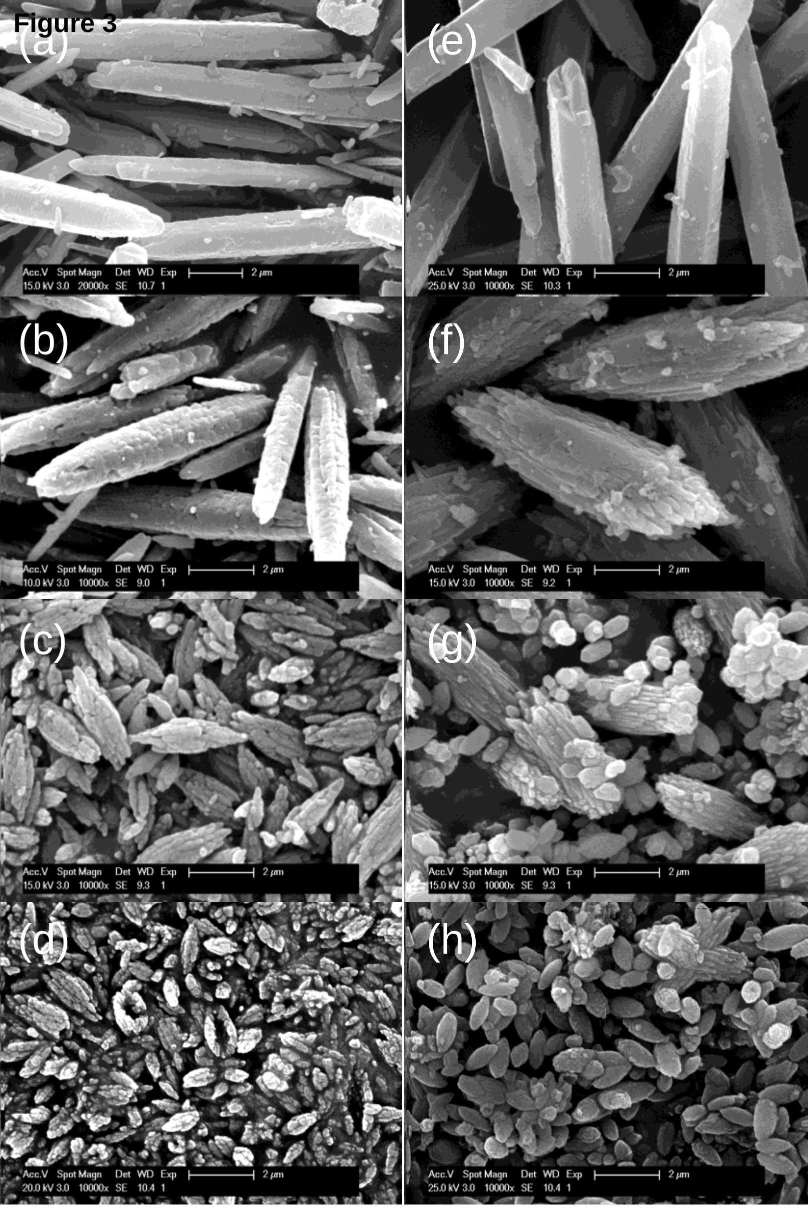
(a)
Acc.V Spot Magn Det WD Exp 2 µm
15.0 kV 3.0 20000x SE 10.7 1
(b)
Acc.V Spot Magn Det WD Exp 2 µm
10.0 kV 3.0 10000x SE 9.0 1
(c)
Acc.V Spot Magn Det WD Exp 2 µm
15.0 kV 3.0 10000x SE 9.3 1
(d)
Acc.V Spot Magn Det WD Exp 2 µm
20.0 kV 3.0 10000x SE 10.4 1
(e)
Acc.V Spot Magn Det WD Exp 2 µm
25.0 kV 3.0 10000x SE 10.3 1
(f)
Acc.V Spot Magn Det WD Exp 2 µm
15.0 kV 3.0 10000x SE 9.2 1
(g)
Acc.V Spot Magn Det WD Exp 2 µm
15.0 kV 3.0 10000x SE 9.3 1
(h)
Acc.V Spot Magn Det WD Exp 2 µm
25.0 kV 3.0 10000x SE 10.4 1

Figure 4

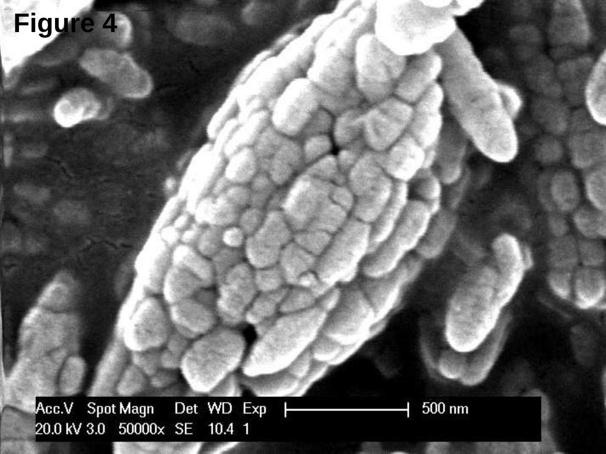

Figure 5

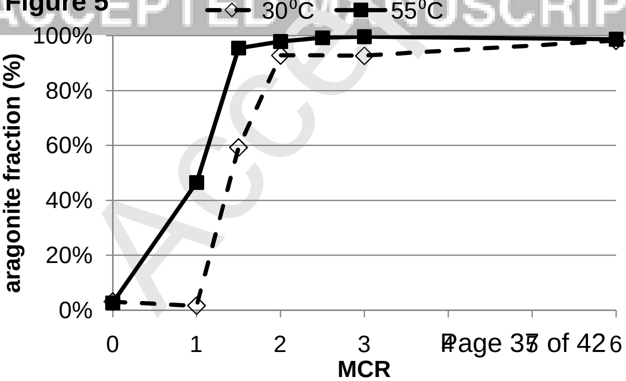

Figure 6

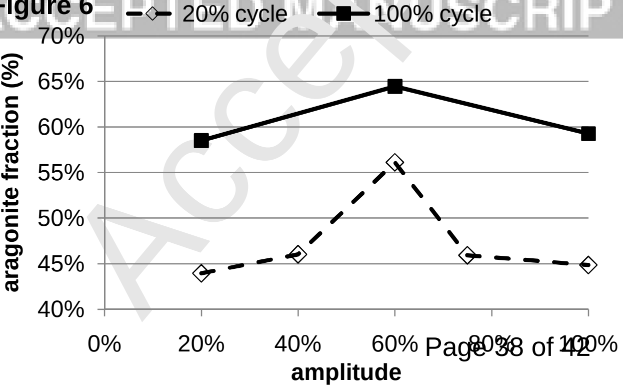

20% cycle
100% cycle
70%
65%
60%
55%
50%
45%
40%
aragonite fraction (%)
0%
20%
40%
60%
80%
100%
amplitude

Figure 7

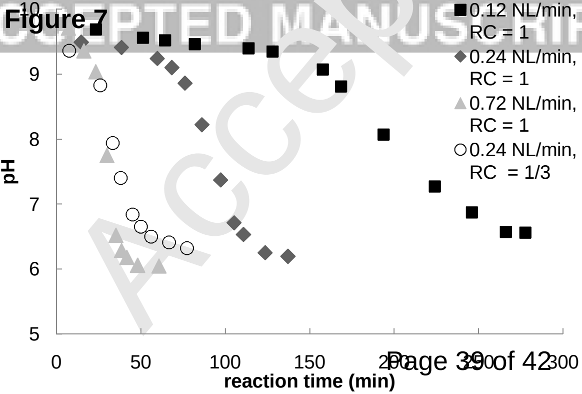
pH
10
9
8
7
6
5
0
50
100
150
200
250
300
reaction time (min)
■ 0.12 NL/min, RC = 1
◆ 0.24 NL/min, RC = 1
▲ 0.72 NL/min, RC = 1
○ 0.24 NL/min, RC = 1/3

Figure 8

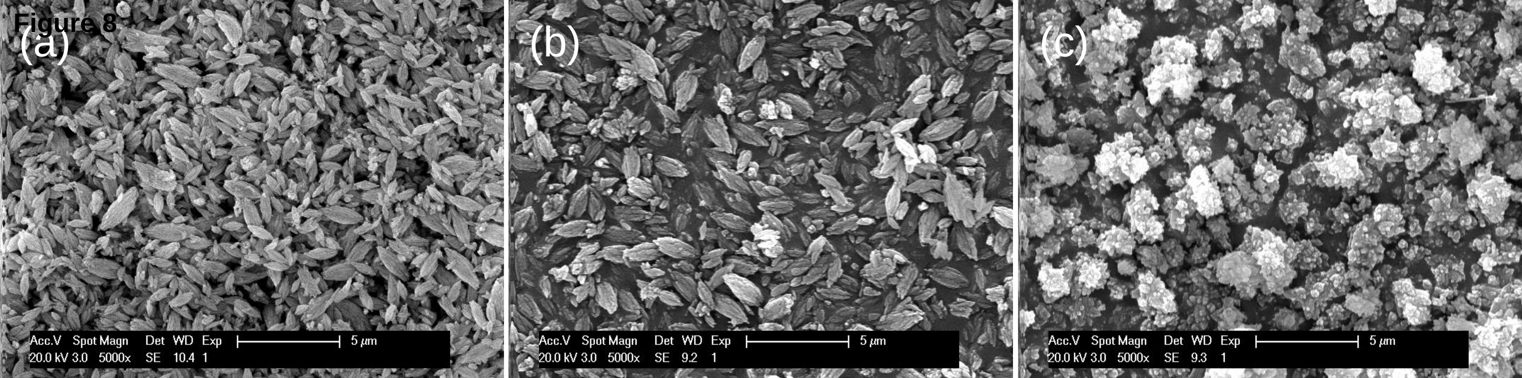
(a)
Acc.V Spot Magn Det WD Exp
5 µm
20.0 kV 3.0 5000x SE 10.4 1
(b)
Acc.V Spot Magn Det WD Exp
5 µm
20.0 kV 3.0 5000x SE 9.2 1
(c)
Acc.V Spot Magn Det WD Exp
5 µm
20.0 kV 3.0 5000x SE 9.3 1

Figure 9

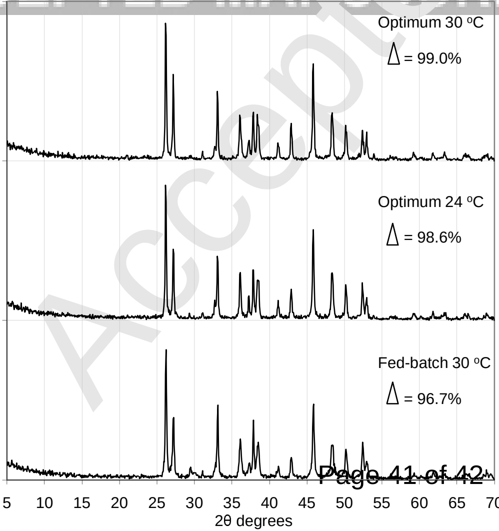
Optimum 30 °C
∆ = 99.0%
Optimum 24 °C
∆ = 98.6%
Fed-batch 30 °C
∆ = 96.7%
5
10
15
20
25
30
35
40
45
50
55
60
65
70
2θ degrees

Figure 10

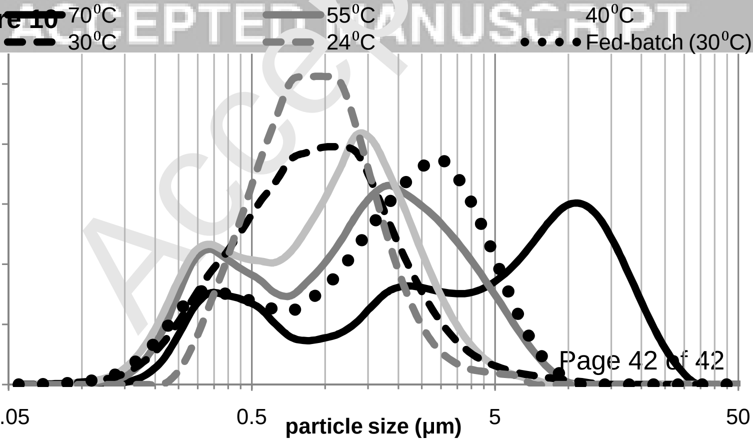
70°C
55°C
40°C
30°C
24°C
Fed-batch (30°C)
volume %
0
2
4
6
8
10
particle size (µm)
0.05
0.5
5
50